GSA DATA REPOSITORY ITEM 2006152

APPENDIX 1: SAMPLE PREPARATION AND ANALYTICAL TECHNIQUES

Apatite (U-Th)/He thermochronometry

We collected modern fluvial sediment from Inyo Creek and Lone Pine Creeks where they exit the mountain front, three bedrock samples from each of the three plutons that outcrop in these catchments, and glacial sediment stored in a moraine low in the Lone Pine Creek catchment (see Fig. 2 for sample locations). Apatites were separated from these samples using conventional heavy-liquid and magnetic separation techniques and were sieved to a minimum dimension of 100-150 μm. We hand picked euhedral and inclusion-free apatite grains under a 120x binocular microscope with cross polars (Fig. DR1), measured them for α emission correction (Farley et al., 1996), loaded them into Pt capsules, and out-gassed them under a laser at 1100 ºC for 5 minutes (House et al., 2000). Evolved helium was spiked with ^{3}He, cryogenically concentrated and purified, and the ^{4}He/^{3}He ratio measured on a quadrupole mass spectrometer. After out-gassing, the grains were retrieved, dissolved in HNO_3, spiked with ^{235}U and ^{230Th}, and Th and U isotope ratios analyzed by ICP-MS.

AHe ages for the bedrock and modern sediment samples are shown in Tables DR1 and DR2, respectively. We did not date any apatites from the moraine, but note that it contains numerous high-quality grains suitable for dating (Fig. DR1C).

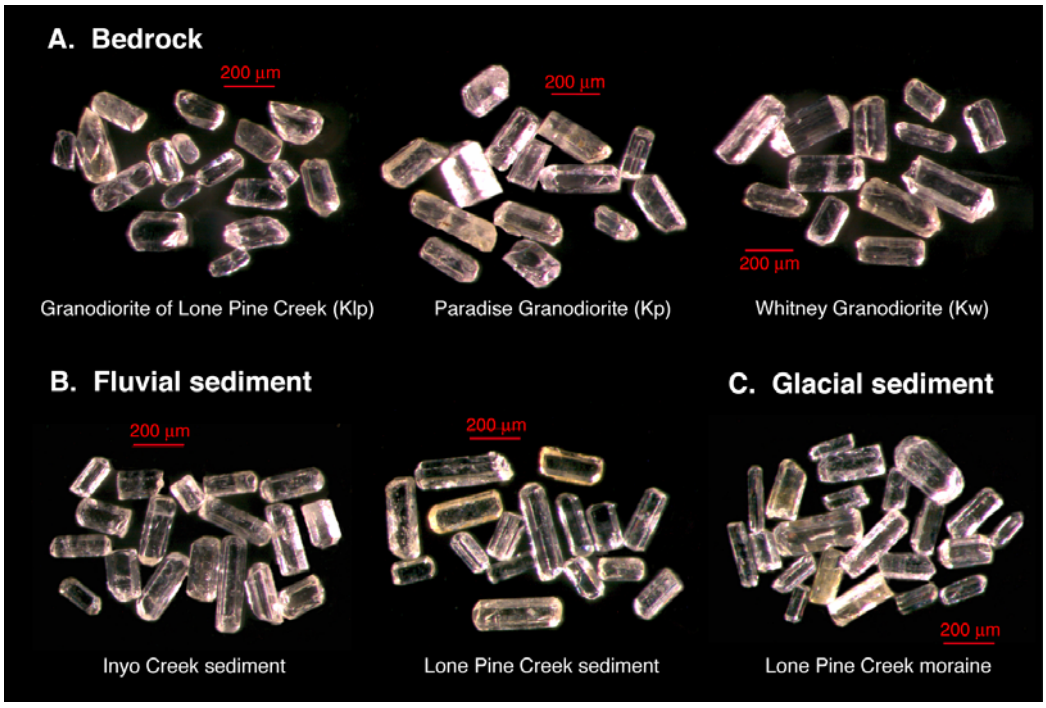

Figure DR1. Photomicrographs of representative apatite grains from the study area. A) Apatites from each of the three plutons outcropping in Inyo Creek and Lone Pine Creek catchments. B) Apatites from sediment collected from Inyo and Lone Pine Creeks. C) Apatites from a glacial moraine in the Lone Pine Creek catchment (Fig. 2). All grains show size and euhedral morphology appropriate for α-ejection correction (Farley et al., 1996).

Constructing and comparing predicted and measured AHe PDFs

We describe the distribution of AHe cooling ages in a detrital sample in terms of a synoptic probability density function (PDF), defined as the normalized summation of the individual grain age measurements (t_m) and their associated 1σ Gaussian uncertainties (σ_{tm}):

$$PDF = \frac{\sum_{i=1}^{n} \left(\frac{1}{\sigma_{t_m}\sqrt{2\pi}} \right) e^{\frac{-(t-t_m)^2}{2\sigma_{t_m}^2}}}{n} \qquad (1)$$

where n is the number of grains analyzed (Hodges et al., 2005; Ruhl and Hodges, 2005). We used a similar approach to construct predicted PDFs of AHe age distributions; we first fit a line through the age-elevation transect data (House et al., 1997, and this study), and then using this relationship to assign a "model" AHe age to each elevation in a 30 m digital elevation model (DEM) of the catchment. We assume that there is no lateral variation in bedrock AHe ages across our small study area (though see below). As described in the text, our assigned 1σ uncertainty on the detrital AHe ages is 11%, based on the reproducibility of bedrock AHe ages collected from the ridge between Inyo Creek and Lone Pine Creek (Fig. 2). The bedrock AHe ages of House et al. (1997) were determined using a slightly different technique (groups of apatites rather than single grains) and thus their reported 1σ uncertainty is less than 11%. We conservatively used the 11% value in generating the PDFs.

Following Ruhl and Hodges (2005), we statistically compared the predicted and measured PDFs using a two-sample Kuiper Equality test (Kuiper, 1962; Press et al., 1992). We then set up a Monte Carlo routine in which n ages (n = 52 for Inyo Creek, n = 54 for Lone Pine Creek) were randomly selected from the predicted PDF and compared with the measured PDF using the Kuiper test. We ran the Monte Carlo routine 10,000 times and compiled the test statistics. We repeated the process for n = 100 ages selected from the predicted PDF. Mean Kuiper test statistics for the predicted and measured PDF comparisons are shown in Table DR3. These tests indicate that the measured PDF for the Inyo Creek catchment is statistically indistinguishable from the predicted PDF (H = 1), i.e., the two distributions are the same at the 95% confidence interval. In contrast, the measured PDF for the Lone Pine Creek catchment is statistically different from the predicted PDF (H = 0).

Assessing the quality of AHe ages

In detrital samples from both Inyo and Lone Pine Creeks, there are several "outlier" AHe ages, i.e., ages that are outside (>2σ) the range predicted by the hypsometry and age-elevation relationship. How to explain these outliers? The U concentration in the analyzed apatite grains is sufficiently distinctive to indicate pluton source. Specifically, the Lone Pine Creek granodiorite has a much higher [U] than either the Whitney or Paradise granodiorites (Fig. DR2). According to the geologic map (Fig. 2) and the bedrock age-elevation transect (Fig. 4A), the two youngest samples from the Lone Pine Creek detrital sample (02TELP05-025 and 02TELP05-041) have ages

consistent with derivation from either the Lone Pine Creek granodiorite (<20 Ma). However, their low [U] is consistent with either the Whitney or Paradise granodiorites, which should yield ages ≥30 Ma. These two grains must be giving erroneous ages, likely due to age resetting by wildfires. Both catchments are presently sparsely vegetated, and were apparently even less vegetated during glacial times (Woolfenden, 2003). This reduces the potential for wildfire resetting but does not eliminate entirely, especially for the lower parts of the catchment. Accordingly, we omitted these two ages from our analyses.

There are a number of apatites in the Inyo Creek detrital sample that derive from the Lone Pine Creek granodiorite (Fig. DR2). These grains are clearly the youngest (<~32 Ma), consistent with their low elevation source (Fig. 2). However, the situation is different in the detrital sample from Lone Pine Creek. Based on high [U], there appears to be only a single grain (02TELP05-013) that derives from the Lone Pine Creek granodiorite, with an age of ~40 Ma. This age is inconsistent with the mapped distribution of this pluton (Fig. 2); perhaps it is a grain with unusual chemistry from either the Whitney or Paradise granodiorites, or, less likely, it derives from an unmapped exposure of the Lone Pine Creek granodiorite or a similar pluton.

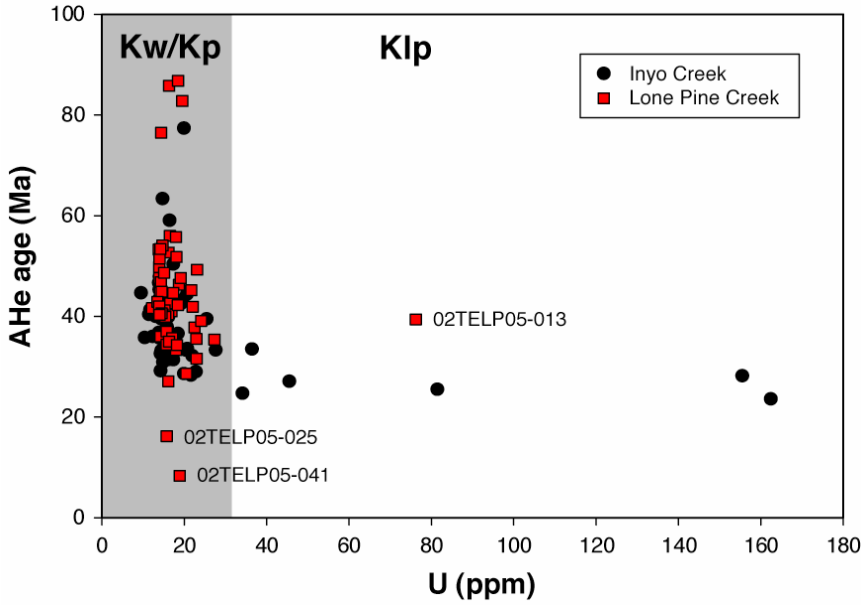

Figure DR2. Plot of U concentration versus AHe age. Gray shaded area represents the U concentration of the Whitney (Kw) and Paradise (Kp) granodiorites, white area the Lone Pine Creek granodiorite (Klp). Two youngest AHe ages from Lone Pine Creek have [U] consistent with either the Kw or Kp but AHe ages consistent with lower elevation Klp outcrop, suggesting forest fire resetting.

Fig. DR2 also illustrates the presence of 1-2 old outliers in both the Inyo and Lone Pine creek catchments. These may reflect apatites that contained non-detectable inclusions, or they may indicate the presence of minor three-dimensionality (i.e., lateral variation) in bedrock AHe ages across the catchments. This latter effect would result from isotherms that were not strictly horizontal during cooling, probably due to

paleotopography. If so, there may be unsampled outcrop areas with AHe ages older than the summit of Mt. Whitney. Such lateral variation in bedrock AHe ages has been well documented in the Sierra Nevada west and south of the study area (House et al., 1998; Clark et al., 2005). However, our bedrock samples collected from the ridge between Inyo and Lone Pine Creeks follow the trend established by those samples collected by House et al. (1997) from the Lone Pine Creek catchment (Fig. 4A), suggesting that lateral variation in ages is minor across our very small study area. Furthermore, this variation is within the 11% 1σ uncertainty of our bedrock ages, and is thus accounted for in our statistical comparisons.

Cosmogenic ^{10}Be-based catchment erosion rate

We separated out ~200 g of Inyo Creek sediment for cosmogenic ^{10}Be analysis. The sediment was crushed and sieved to 0.25-0.85 mm, and quartz purified by selective chemical dissolution (Kohl and Nishiizumi, 1992). The sample was spiked with ~0.3 mg ^{9}Be carrier (^{10}Be/^{9}Be=6×10^{-15}). The quartz was then dissolved in concentrated HF and HNO_3, fluorides expelled with aqua regia fuming, and Be separated and purified by oxalic acid-based ion exchange chromatography and selective precipitation. BeOH precipitate was oxidized at 1000°C, mixed with Nb powder, and packed into a stainless steel cathode. The ^{10}Be/^{9}Be ratio was measured by accelerator mass spectrometry at the Purdue Rare Isotope Measurement (PRIME) laboratory. Results are shown in Table DR4.

Calculating catchment-averaged erosion rate requires a mean nuclide production (neutron and muon) rate for the catchment. To determine this we first calculated a local production rate, scaled for latitude, altitude (as expressed by atmospheric pressure; Stone, 2000), and topographic shielding (Dunne et al, 1999), for each pixel of a 30 m DEM of the Inyo Creek catchment. In addition, we scaled the production rate for annual snow shielding using monthly local snowpack data (http://cdec.water.ca.gov) and modifying the formulation of Gosse and Phillips (2001):

$$S = \frac{1}{n}\sum_{i=1}^{n} e^{-(z_{snow,i})\rho_{snow,i}/\Lambda)} \tag{2}$$

where S is the snow shielding factor, $z_{snow,i}$ is the monthly average snow height (cm) above the ground surface, and $\rho_{\sigma now,i}$. is the snowpack density. The interval of summation, i, was one month, and n, the total length of the summation time, was 12 (i.e., 1 year). We used snowpack data converted to snow water equivalent, so in this case $z_{snow,i}$ is the monthly average snow water equivalent height (cm) and $\rho_{\sigma now,i}$ is the density of water.

We calculated the catchment erosion rate (ε) by iteratively solving Eq. 3 (Granger et al., 2001):

$$N = \frac{P_n}{\tau^{-1} + \rho\varepsilon(\Lambda^{-1})} + \frac{YA_1}{\tau^{-1} + \rho\varepsilon(L_1{}^{-1})} + \frac{YA_2}{\tau^{-1} + \rho\varepsilon(L_2{}^{-1})} + \frac{B}{\tau^{-1} + \rho\varepsilon(L_3{}^{-1})} \tag{3}$$

where P_n is the sea level, high latitude ^{10}Be production rate at the surface due to nucleon spallation (5.1 ± 0.3 atm/g/yr; Stone, 2000) scaled as described above, τ is the ^{10}Be meanlife (2.18 ± 0.09 Ma; Middleton et al., 1993), ρ is the bedrock density (2.7 g/cm^3), Λ is the neutron penetration depth for nucleons (160 g/cm^2; Masarik and Reedy, 1995), A_1 and A_2 are the production rates of negative muons (170.6 μ^-/g/yr and 36.8 μ^-/g/yr, respectively; Granger and Smith, 2000), Y is the yield of ^{10}Be per negative muon (5.6×10^{-4} atm/μ^-; Heisinger, 1998), B is the production rate of ^{10}Be due to fast muons (0.026 atm/g/yr; Granger and Smith, 2000), and L_1, L_2, and L_3 are the penetration depths for muon reactions (738.6, 2688, and 4360 g/cm^2, respectively; Granger and Smith, 2000).

Additional references

Dunne, J., Elmore, D., and Muzikar, P., 1999, Scaling factors for the rates of production of cosmogenic nuclides for geometric shielding and attenuation at depth on sloped surfaces: Geomorphology, v. 27, p. 3-11.

Farley, K.A., Wolf, R.W., and Silver, L.T., 1996, The effects of long-stopping distances on (U-Th)/He ages: Geochemica et Cosmochemica Acta, v. 60, p. 4223-4229.

Granger, D.E., and Smith, A.L., 2000, Dating buried sediments using radioactive decay and muogenic production of ^{26}Al and ^{10}Be: Nuclear Instruments and Methods in Physics Research B, v. 172, p. 822-826.

Granger, D.E., Riebe, C.S., Kirchner, J.W., and Finkel, R.C., 2001, Modulation of erosion on steep granitic slopes by boulder armoring, as revealed by cosmogenic ^{26}Al and ^{10}Be: Earth and Planetary Science Letters, v. 186, p. 269-281.

Gosse, J.C., and Phillips, F.M., 2001, Terrestrial in situ cosmogenic nuclides: Theory and applications: Quaternary Science Reviews, v. 20, p. 1475-1560.

Heisinger, B.P., 1998, Myonen-induzierte Producktion von Radionukliden. Ph.D. thesis, Technische Universitat Munchen.

Hodges, K.V., Ruh, K.W., Wobus, C.W., and Pringle, M.S., 2005, ^{40}Ar/^{39}Ar Thermochronology of Detrital Minerals, *in* Reiners, P.W., and Ehlers, T.A., eds., Low-Temperature Thermochronology: Techniques, Interpretations, and Applications: Reviews in Mineralogy and Geochemistry, v. 58, p. 239-257.

House, M.A., Wernicke, B.P., and Farley, K.A., 1998, Dating topography of the Sierra Nevada, California, using apatite (U-Th)/He ages: Nature, v. 396, p. 66 – 69.

House, M.A., Farley, K.A., and Stockli, D., 2000, Helium chronometry of apatite and titanite using Nd-YAG laser heating: Earth and Planetary Science Letters, v. 183, p. 365-368.

Kohl, C.P., and Nishiizumi K., 1992, Chemical isolation of quartz for measurement of *in-situ*-produced cosmogenic nuclides: Geochimica et Cosmochimica Acta, v. 56, p. 3583-3587.

Kuiper, N.H., 1962, Tests concerning random points on a circle: Proceedings of the Koninklijke Nederlandse Akademie van Wetenschappen, v. 63, p. 38-47.

Masarik, J., and Reedy, R.C., 1995, Terrestrial cosmogenic nuclide production systematics calculated from numerical simulations: Earth and Planetary Science Letters, v. 136, p. 381-395.

Press, W.H., Teukolsky, S.A., Vetterling, W.T., and Flannery, B.P., 1992, Numerical Recipes in C: The Art of Scientific Computing, 994 pp., Cambridge University Press, New York.

Stone, J.O., 2000, Air pressure and cosmogenic isotope production: Journal of Geophysical Research, v. 105, p. 23,753-23,759.

Woolfenden, W.B., 2003, A 180,000-year pollen record from Owens Lake, CA: Terrestrial vegetation change on orbital scales: Quaternary Research, v. 59, p. 430-444.

Table DR1. Bedrock apatite (U-Th)/He data from Inyo Creek and Lone Pine Creek catchments

Sample	Length (μm)	Diameter (μm)	U (ppm)	Th (ppm)	He (nmol/g)	F_t	Raw age (Ma)	Corrected age (Ma)*	±1σ (Ma)
Whitney Granodiorite			Elev. 3088 m		Lat. 36.57626°N		Long. 118.22069°W		
05GS01Kw-001	200	95	16.5	46.1	5.4	0.72	36.2	50.1	
05GS01Kw-002	194	86	18.4	49.7	4.1	0.70	25.1	36.0	
05GS01Kw-003	193	74	26.1	76.6	6.1	0.66	25.2	38.1	
05GS01Kw-004	231	120	13.5	38.4	3.7	0.77	29.9	38.6	
05GS01Kw-005	303	119	17.4	59.4	6.2	0.78	36.5	46.9	
							Mean	41.9	6.1
Paradise Granodiorite			Elev. 2839 m		Lat. 36.58050°N		Long. 118.21688°W		
05GS02Kp-001	174	90	28.7	83.6	6.0	0.71	22.9	32.4	
05GS02Kp-002	152	90	15.9	43.0	2.9	0.73	20.6	28.0	
05GS02Kp-004	159	112	16.1	44.1	3.2	0.73	22.0	30.1	
05GS02Kp-005	176	90	16.4	44.7	3.4	0.70	23.3	33.1	
							Mean	30.9	2.3
Granodiorite of Lone Pine Creek			Elev. 2320 m		Lat. 36.58819°N		Long. 118.20758°W		
05GS03Klp-001	278	167	54.2	65.5	10.3	0.84	27.1	32.4	
05GS03Klp-002	137	92	92.9	149.7	13.2	0.71	19.0	26.9	
05GS03Klp-003	201	83	172.2	269.9	23.1	0.70	18.0	25.9	
05GS03Klp-004	207	108	66.5	68.4	8.7	0.76	19.4	25.6	
05GS03Klp-005	152	105	58.6	68.8	8.1	0.74	19.9	26.8	
							Mean	27.5	2.8

* Corrected for alpha ejection after Farley et al. (1996)

Table DR2. Detrital apatite (U-Th)/He data from Inyo Creek and Lone Pine Creek catchments

Sample	Length (μm)	Diameter (μm)	U (ppm)	Th (ppm)	He (nmol/g)	F_t	Raw age (Ma)	Corrected age (Ma)*	±1σ (Ma)†
Inyo Creek	Elev. 1950 m		Lat. 36.59243°N		Long. 118.19755°W				
02TEIC01-001	464	127	10.4	34.5	2.9	0.79	28.5	35.8	3.9
02TEIC01-002	420	136	14.1	45.3	4.6	0.81	34.3	42.5	4.6
02TEIC01-003	233	118	14.8	43.2	3.2	0.77	23.8	30.9	3.3
02TEIC01-004	276	137	17.9	52.2	5.7	0.80	34.7	43.4	4.7
02TEIC01-007	310	137	13.9	45.6	4.9	0.80	36.4	45.3	4.9
02TEIC01-008	195	126	16.0	40.5	3.3	0.77	24.0	31.4	3.3
02TEIC01-010	381	146	16.1	41.2	4.6	0.82	32.6	39.9	4.3
02TEIC01-011	273	131	17.3	55.3	4.1	0.79	24.9	31.4	3.4
02TEIC01-014	209	152	14.4	35.6	3.2	0.81	25.9	33.2	3.4
02TEIC01-015	297	120	27.6	78.8	6.5	0.78	25.9	33.3	3.6
02TEIC01-016	296	217	11.7	29.1	3.6	0.86	35.8	41.3	4.5
02TEIC01-017	232	132	25.4	47.4	6.2	0.79	31.3	39.5	4.3
02TEIC01-018	269	160	13.8	43.1	5.0	0.82	38.5	46.7	5.0
02TEIC01-019	228	112	19.9	54.4	3.9	0.76	21.8	28.6	3.1
02TEIC01-020	339	107	20.6	61.6	6.4	0.76	33.7	44.4	4.8
02TEIC01-022	232	161	21.9	24.6	4.0	0.83	26.6	32.2	3.5
02TEIC01-023	250	134	16.0	47.3	4.3	0.79	28.9	36.4	3.9
02TEIC01-024	196	139	36.4	63.9	7.5	0.80	26.7	33.5	3.6
02TEIC01-025	161	128	15.4	47.9	3.7	0.77	25.5	33.0	3.6
02TEIC01-026	352	117	13.8	40.2	3.6	0.78	28.6	36.8	4.0
02TEIC01-027	202	139	14.4	47.6	4.4	0.79	31.4	39.5	4.3
02TEIC01-028	204	105	17.3	42.3	5.6	0.74	37.5	50.4	5.4

02TEIC01-029	302	77	16.2	47.3	3.6	0.68	24.0	35.2	3.8
02TEIC01-030	373	121	14.2	40.4	3.0	0.79	23.0	29.2	3.2
02TEIC01-031	191	115	15.5	45.4	3.5	0.76	24.9	32.8	3.5
02TEIC01-032	134	111	19.9	55.6	10.3	0.74	57.4	77.4	8.4
02TEIC01-033	164	116	18.4	48.7	4.5	0.76	27.7	36.6	4.0
02TEIC01-034	338	181	20.7	52.2	5.1	0.85	28.5	33.6	3.6
02TEIC01-035	144	103	22.8	52.2	4.0	0.73	21.2	29.0	3.1
02TEIC01-036	155	104	14.0	41.4	4.5	0.73	35.1	47.9	5.2
02TEIC01-037	314	129	81.4	124.2	12.2	0.80	20.3	25.5	2.8
02TEIC01-038	226	170	21.6	43.3	4.1	0.83	23.6	28.3	3.1
02TEIC01-039	444	171	16.9	50.6	4.8	0.84	30.4	36.0	3.9
02TEIC01-041	324	107	16.4	49.2	6.8	0.76	44.9	59.1	6.4
02TEIC01-042	175	114	20.3	49.2	4.4	0.76	25.2	33.3	3.6
02TEIC01-043	176	132	155.5	106.4	21.9	0.79	22.3	28.2	3.0
02TEIC01-044	177	96	16.5	38.5	3.3	0.72	23.3	32.3	3.5
02TEIC01-045	231	119	162.4	134.1	19.4	0.78	18.4	23.6	2.6
02TEIC01-046	267	99	45.5	74.9	6.9	0.74	20.1	27.1	2.9
02TEIC01-047	288	161	34.1	68.4	5.6	0.83	20.5	24.7	2.7
02TEIC01-048	187	141	11.4	34.6	3.4	0.79	32.0	40.4	4.4
02TEIC01-049	240	144	16.7	40.9	5.1	0.81	35.7	44.2	4.8
02TEIC01-050	272	125	12.3	32.6	3.1	0.79	28.3	36.0	3.9
02TEIC01-051	224	163	13.9	37.3	3.6	0.82	29.4	35.7	3.9
02TEIC01-052	174	138	14.2	38.2	3.2	0.79	25.7	32.6	3.5
02TEIC01-053	281	107	16.2	43.2	3.7	0.76	25.6	33.8	3.7
02TEIC01-054	355	160	13.0	35.8	3.8	0.83	32.9	40.0	4.3
02TEIC01-055	291	164	14.7	43.3	7.1	0.83	52.6	63.4	6.8
02TEIC01-056	268	157	19.1	50.0	5.9	0.82	34.9	42.5	4.6
02TEIC01-057	254	166	13.9	45.8	4.8	0.83	36.0	43.5	4.7
02TEIC01-058	367	118	15.8	38.2	4.0	0.78	29.6	37.9	4.1
02TEIC01-059	152	107	9.5	29.7	3.0	0.76	33.9	44.7	4.8
Lone Pine Creek	Elev. 1950 m		Lat. 36.57825°N		Long. 118.21269°W				
02TELP05-001	206	99	16.9	45.6	4.9	0.73	32.5	44.3	4.8
02TELP05-002	210	147	14.2	41.2	3.8	0.80	29.0	36.0	3.9
02TELP05-003	288	141	27.3	41.1	5.8	0.81	28.6	35.4	3.8
02TELP05-004	331	135	13.9	43.3	5.0	0.80	38.2	47.6	5.1
02TELP05-005	284	112	14.1	40.3	4.4	0.76	34.5	45.1	4.9
02TELP05-006	180	100	18.0	47.9	3.9	0.73	24.3	33.3	3.6
02TELP05-007	182	141	16.9	39.0	4.6	0.80	32.6	41.0	4.4
02TELP05-008	282	114	16.6	57.3	5.3	0.77	32.6	42.6	4.6
02TELP05-009	249	135	16.5	53.7	7.1	0.80	44.6	56.0	6.0
02TELP05-010	177	107	13.8	47.7	5.4	0.74	39.6	53.3	5.8
02TELP05-011	122	115	12.2	37.8	3.5	0.74	30.9	41.6	4.5
02TELP05-012	150	128	16.2	38.6	5.6	0.77	40.7	52.7	5.7
02TELP05-013	210	104	76.2	85.7	15.5	0.75	29.5	39.4	4.3
02TELP05-014	245	88	22.9	48.1	4.7	0.71	25.2	35.5	3.8
02TELP05-015	224	109	14.7	47.4	5.8	0.75	40.8	54.1	5.8
02TELP05-016	345	126	16.1	53.4	5.0	0.79	32.0	40.4	4.4
02TELP05-017	196	88	14.3	48.5	4.6	0.70	32.8	46.8	5.1
02TELP05-018	280	129	13.9	43.1	5.2	0.79	39.4	49.8	5.4
02TELP05-019	320	93	20.5	50.6	3.7	0.73	20.9	28.6	3.1
02TELP05-020	203	100	23.1	60.4	7.1	0.70	34.7	49.3	5.3
02TELP05-021	185	93	14.5	50.2	4.6	0.71	32.1	44.9	4.8
02TELP05-022	113	101	18.7	59.1	5.9	0.71	33.0	46.3	5.0
02TELP05-023	230	124	19.5	54.4	11.4	0.78	64.6	82.8	8.9
02TELP05-024	339	82	14.0	41.8	4.7	0.70	36.0	51.5	5.6

02TELP05-025	287	138	15.7	41.2	1.8	0.80	13.0	16.2	1.7
02TELP05-026	365	130	22.0	62.1	6.7	0.80	33.5	41.9	4.5
02TELP05-028	301	123	15.2	47.7	4.7	0.78	32.4	41.2	4.5
02TELP05-029	238	104	16.3	50.9	9.9	0.75	64.2	85.8	9.3
02TELP05-030	290	124	13.5	41.3	4.3	0.78	33.7	42.9	4.6
02TELP05-031	291	103	23.0	62.8	4.9	0.75	23.7	31.6	3.4
02TELP05-032	287	90	16.1	41.9	2.8	0.72	19.5	27.1	2.9
02TELP05-033	174	77	13.9	43.0	3.7	0.67	28.0	42.0	4.5
02TELP05-034	296	94	17.3	51.3	5.2	0.73	32.7	44.7	4.8
02TELP05-035	339	109	18.0	57.0	7.3	0.76	42.6	55.8	6.0
02TELP05-036	283	126	18.1	54.6	6.9	0.79	40.8	51.8	5.6
02TELP05-037	167	116	15.7	53.3	4.3	0.76	28.0	37.0	4.0
02TELP05-038	138	108	21.7	47.3	5.9	0.73	33.2	45.2	4.9
02TELP05-039	212	103	17.1	48.7	4.1	0.74	26.5	35.7	3.9
02TELP05-040	150	95	14.7	48.3	4.1	0.71	28.7	40.4	4.4
02TELP05-041	155	101	18.9	58.7	1.1	0.72	6.0	8.3	0.9
02TELP05-042	160	103	15.1	53.3	5.4	0.73	35.6	48.7	5.3
02TELP05-043	223	127	14.4	40.9	7.9	0.78	59.9	76.5	8.3
02TELP05-044	183	82	19.1	54.4	5.7	0.68	32.6	47.6	5.1
02TELP05-045	180	95	22.5	45.5	4.9	0.72	27.3	37.8	4.1
02TELP05-046	230	115	15.4	52.2	4.6	0.76	30.5	39.9	4.3
02TELP05-047	290	109	14.5	45.2	4.2	0.76	30.9	40.6	4.4
02TELP05-048	258	76	24.1	57.8	5.4	0.68	26.5	39.1	4.2
02TELP05-049	167	94	18.5	51.7	10.4	0.71	62.0	86.8	9.4
02TELP05-050	305	84	18.4	56.3	5.1	0.70	29.7	42.2	4.6
02TELP05-051	419	144	15.7	47.4	4.1	0.82	28.1	34.4	3.7
02TELP05-052	258	110	14.0	46.2	4.2	0.76	30.6	40.3	4.4
02TELP05-053	158	107	14.2	50.0	5.6	0.74	39.4	53.4	5.8
02TELP05-054	310	107	16.3	49.0	4.0	0.76	26.6	35.0	3.8
02TELP05-055	183	89	18.2	45.9	3.8	0.71	24.2	34.3	3.7

* Corrected for alpha ejection after Farley et al. (1996)

† 1σ errors are 11% and represent mean uncertainty on reproducibility of bedrock samples (Table DR1).

Table DR3. Kuiper Equality Test results (alpha = 0.05) for comparisons of predicted and measured PDFs from Inyo Creek and Lone Pine Creek catchments

Sample 1 (Measured PDF)	n1	Sample 2 (Predicted PDF)	n2	*V*	*P*	H
Inyo Creek	52	Inyo Creek	52	0.1946	0.7133	1 (0.995)
Inyo Creek	52	Inyo Creek	100	0.1868	0.6230	1 (0.996)
Lone Pine Creek	54	Lone Pine Creek	54	0.4234	0.0074	0 (0.030)
Lone Pine Creek	54	Lone Pine Creek	100	0.4206	0.0007	0 (0.001)

Kuiper statistic *V* and significance level *P* of an observed value of *V* are calculated for each comparison between sample 1, defined by n1 measured ages, and sample 2, defined by n2 ages selected randomly from the predicted PDF (as a disproof of the null hypothesis that the measured and predicted PDFs are the same). H = 1 indicates that the null hypothesis cannot be disproved at significance level alpha, i.e., the samples are statistically similar; H = 0 indicates that samples 1 and 2 are different at significance level alpha. *V* and *P* are mean values of 10,000 Monte Carlo simulations.

Table DR4. Cosmogenic ^{10}Be concentration and erosion rate for the Inyo Creek catchment

Sample	Mass quartz (g)	^{10}Be (10^5 atm/g)*	P_{10} (atm/g/yr)†	Erosion rate (mm/yr)	Erosion timescale (yr)
02TEIC01-Be	118.16	1.73 ± 0.01	43.21 ± 3.1	0.24 ± 0.03	3860

* Uncertainty is 1σ analytical uncertainty.

† Mean ^{10}Be production rate determined by calculating the local production rate, assuming a sea level high-latitude production rate of 5.1 ± 0.3 atm/g/yr (Stone, 2000) scaled for latitude, altitude, and topographic and snow shielding, for each pixel of a 30 m catchment DEM. P_{10} error is propagated uncertainty in ^{10}Be production rate (Stone, 2000) and pixel altitude (30 m).